Role of molecular orbital symmetry on the alignment dependence of high-order harmonic generation with molecules

Xiao Xin Zhou,[1,2] X. M. Tong,[1] Z. X. Zhao,[1] and C. D. Lin[1,*]

[1]*J. R. Macdonald Laboratory, Physics Department, Kansas State University, Manhattan, Kansas 66506, USA*
[2]*College of Physics and Electronic Engineering, Northwest Normal University, Lanzhou, Gansu 730070, People's Republic of China*
(Received 4 January 2005; published 2 June 2005)

It is shown that the alignment dependence of the yields of high-order harmonic generation (HHG) from molecules by intense lasers is governed by the orbital symmetry of the outermost electron(s). For N_2, with its outermost σ_g electron, the HHG yield is maximal when the molecules are aligned with the laser polarization direction, in agreement with the recent experiment of Itatani *et al.* [Nature **432**, 867 (2004)]. For O_2, with its outermost π_g electron, the HHG yield peaks when the molecules are aligned at about 45° from the polarization axis. We emphasize that the alignment dependence is determined mostly by the orbital symmetry and weakly on the laser parameters or the species.

The interaction of strong laser pulses with atoms or molecules leads to the generation of high-order harmonics [1–3]. This is one of the most exciting areas in strong-field physics because it serves as a source of high-frequency coherent radiation [4] and of the generation of attosecond pulses [5,6]. While high-order harmonic generation (HHG) has been well studied for atoms, much less has been done for molecules. In particular, few experiments have been performed to examine the dependence of HHG on the alignment of molecules. Marangos and co-workers [7–9] have studied the high-harmonic generation in H_2, N_2, CO_2, and CS_2 by 70-fs high-intensity laser pulses, with and without the presence of another weak laser pulse that was used to align the molecules. They observed enhancement of HHG when the aligning laser is present. To interpret their observations they carried out restricted one-dimensional (1D) and two-dimensional (2D) model calculations, but with only limited success [9]. In a recent paper, Itatani *et al.* [10] reported a detailed alignment dependence study of HHG of N_2 molecules. They used a short weak laser pulse to create a rotational wave packet. When the field-free wave packet rephases at full or half-full rotational periods, the molecules are instantaneously maximally aligned. By using a stronger probe laser with varying polarization direction with respect to the pump laser, they showed that the HHG yields decrease rapidly as the angle between the two polarizations is increased.

In this Rapid Communication we show that the high-order harmonic generation from aligned molecules can be readily calculated quantitatively, and that the alignment dependence is determined mostly by the orbital symmetry of the outermost electron(s) of the molecule. To obtain HHG from first-principle calculations, one has to compute the Fourier components of the time-dependent induced electric dipole moment by solving the time-dependent Schrödinger equation in the laser field. Clearly such calculation is much too complicated for molecules [7,9,11,12]. However, it is well known that HHG is well-explained conceptually by the recollision

model [13,14]: The strong field from the laser ionizes the atom or molecule to create a free electron. The free electron is accelerated by the oscillating laser field and may be driven back to recollide with the ion if the laser is linearly polarized. High-harmonic photons are emitted if the high-energy electron is recombined with the ionic core. The semiclassical version of this model for the high-order harmonic generation is the Lewenstein model and it has been used to obtain the HHG from atoms [15]. In this paper we extend the Lewenstein model to calculate HHG from aligned molecules to highlight the important role of the orbital symmetry of the outermost electron(s) in the high-order harmonic generation with molecules.

According to the Lewenstein model, the time-dependent dipole moment is given by

$$\mathbf{r}(t) = i \int_{-\infty}^{t} dt' \int d^3\mathbf{p}\, a(t)\mathbf{d}^*[\mathbf{p} - \mathbf{A}(t)] \tag{1a}$$

$$\times e^{-iS(\mathbf{p},t,t')} \tag{1b}$$

$$\times \mathbf{d}[\mathbf{p} - \mathbf{A}(t')]\mathbf{E}(t')a(t') + \text{c.c.}, \tag{1c}$$

with the transition dipole matrix element from the ground state $\Psi_i(\mathbf{r})$ to the final state $\mathbf{p}$ by

$$\mathbf{d}(\mathbf{p}) = \langle \mathbf{p}|\mathbf{r}|\Psi_i(\mathbf{r})\rangle, \tag{2}$$

and

$$S(\mathbf{p},t,t') = \int_{t'}^{t} \left(\frac{[\mathbf{p} - \mathbf{A}(t'')]^2}{2} + I_p \right) dt''. \tag{3}$$

In (1c), c.c. stands for complex conjugate, $\mathbf{E}(t)$ and $\mathbf{A}(t)$ are the instantaneous electric field and the vector potential of the laser, respectively, and $a(t)$ is the amplitude of the ground state. Thus the first term in (1c) represents the amplitude of tunneling ionization occurring at time t'. The electron propagates in the laser field from t' to t, and acquires a phase expressed in (1b), and finally recombines with the ion at time t as expressed by (1a). Using the saddle-point approximation

---

*Corresponding author. Email address: cdlin@phys.ksu.edu
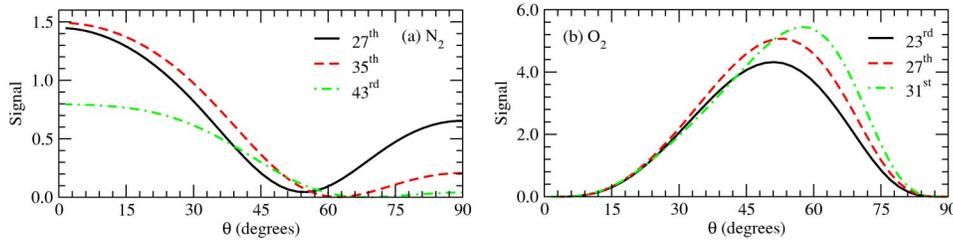
FIG. 1. (Color online) Predicted angular dependence of selective high-order harmonic yields in the plateau region for (a) N_2 and (b) O_2. The angle is between the molecular axis and the laser polarization direction. For the laser parameters used, see text.

for the integration over **p**, Eq. (1) can be simplified to

$$\mathbf{r}(t) = i \int_0^\infty d\tau \left(\frac{\pi}{\epsilon + i\tau/2} \right)^{3/2} \mathbf{d}_x^*[\mathbf{p}_{st}(t,\tau) - \mathbf{A}(t)]$$

$$\times e^{-iS_{st}(t,\tau)} \mathbf{d}[\mathbf{p}_{st}(t,\tau) - \mathbf{A}(t-\tau)]\mathbf{E}(t-\tau)a^*(t)a(t-\tau)$$

$$+ \text{c.c..} \tag{4}$$

Note that in the saddle-point approximation, the induced dipole is in the direction of laser polarization. In this equation, τ is the interval between electron's ionization and recombination, ϵ is a small positive constant, and $\mathbf{p}_{st}(t,\tau) = \int_{t-\tau}^t \mathbf{A}(t')dt'/\tau$ is the momentum at the stationary points of the action S. By approximating $a(t) = \exp(-\int_{-\infty}^t W[t']/2dt')$, we include the depletion of the ground-state population. Here the ionization rate $W(t')$ is evaluated using the alignment-dependent tunneling ionization rates for molecules from the molecular tunneling ionization (MO-ADK) theory [16].

To apply Eq. (4) to HHG from diatomic molecules, we assume that both the molecule and the laser's polarization are on the y-z plane. We choose the molecular axis to be along the z direction and the laser polarization direction makes an angle θ with respect to the z axis. The dipole along the field direction can be explicitly written as

$$|\mathbf{d}| = d_z \cos\theta + d_y \sin\theta, \tag{5}$$

with d_z, d_y the dipole components parallel and perpendicular to the molecular axis, respectively. In Eq. (5), the electric dipole moments, according to the Lewenstein model, are evaluated between the initial ground electronic wave function and a plane wave of momentum **p**. We assume that ionization occurs from the outermost valence electron at the equilibrium internuclear separation and the electronic wave functions are obtained from the GAMESS code [17]. It is clear that Eq. (4) can be extended to polyatomic molecules as well. Once the time-dependent dipole moment is calculated from Eq. (4), its Fourier transform is evaluated to give the HHG spectra.

Since the Lewenstein model is an approximate theory, we have first checked its region of validity for atomic hydrogen by comparing with the HHG calculated from directly solving the time-dependent Schrödinger equation [18]. It was found that the HHGs predicted from the Lewenstein model are too low for the low harmonics, but the predictions for the higher harmonics in the plateau region are quite accurate. This conclusion is in agreement with previous experiences [19]. We will use the Lewenstein model to predict the high-order harmonic generation from aligned molecules in the plateau region only. No attempt will be made for the lower harmonics where other corrections have to be included [20]. Since accurate initial molecular wave functions are used in the calculation and no additional assumptions were made beyond the Lewenstein model, the role of molecular orbitals on HHG and the alignment dependence can be evaluated.

In Fig. 1 we first show in the upper panel the angular dependence of the yields of the 27th, 35th, and 43rd harmonics for N_2 molecules fixed in space. On the lower panel similar angular dependence for the 23rd, 27th, and 31st harmonics from O_2 are compared. The strength of each $(2n+1)$th harmonic was obtained by integrating over the intensity within the energy between the $2n$th and $(2n+2)$th order. The peak laser intensity used was 3×10^{14} W/cm^2 for N_2 and 2×10^{14} W/cm^2 for O_2 respectively, and the pulse duration was 30 fs. For these harmonics in the plateau region, the angular dependence among the different harmonics does not change too much. On the other hand, the angular dependence of the harmonics between N_2 and O_2 differs drastically. For N_2, the HHG yield is highest when the molecule is aligned in the direction of the laser polarization. For O_2, the HHG yield is maximum when the molecule is making an angle near 45° with respect to the polarization axis.

This striking contrast in the alignment dependence of HHG between N_2 and O_2 molecules is the latest example of how the orbital symmetry of the highest occupied molecular orbital (HOMO) is reflected in the strong field physics involving molecules. It was well established in early experiments [21,22] that tunneling ionization rates depend sensitively on the binding energy of the target. For Ar and N_2, they have nearly identical binding energies and their ionization rates were shown to be comparable [21]. However, this is not the case between Xe and O_2. Even though they have nearly identical binding energies, it is much more difficult to ionize O_2 than Xe. Thus it was coined that O_2 molecules exhibit ionization suppression. Consequently, O_2 has higher saturation intensity and as a result, it has higher harmonic cutoff order [23], as compared to Xe. It turns out that ionization suppression is very common in the strong field ionization of molecules, including complex polyatomic molecules [24].

The ionization suppression was interpreted in terms of the interference model by Muth-Bohm *et al.* [25]. They showed that if the molecular orbital is a symmetric combination of the atomic orbitals from the two centers, as in N_2, the ionization rate will not show suppression. If it is an antisymmetric combination of atomic orbitals as in O_2, then it will show ionization suppression. The importance of the symmetry properties of molecular orbitals in strong-field physics was further exhibited more clearly by the tunneling ionization theory of molecules by Tong *et al.* [16] where they showed that the ionization rates for molecules depend directly on the
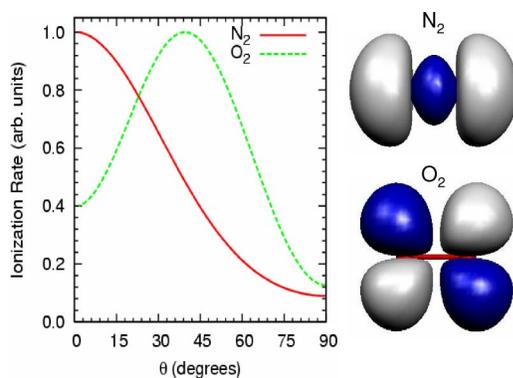
FIG. 2. (Color online) Angular dependence of the ionization rates for N_2 and O_2 calculated from the MO-ADK theory, and plots of the σ_g orbital of N_2 and the π_g orbital of O_2.

electron density of the HOMO in the direction of the laser's polarization. Since the HOMO of N_2 is a σ_g orbital, it has maximum electron density along the direction of the internuclear axis. Thus ionization rate is maximum when N_2 is aligned in the laser's polarization direction. For O_2, its HOMO is a π_g orbital that has a nodal plane along the internuclear axis. Thus when O_2 is aligned in the laser's polarization direction, the ionization rate along that direction is a minimum. Since the HHG has to start with tunneling ionization, at $\theta = 0^\circ$ the HHG predicted for N_2 will be a maximum and for O_2 will be a minimum. Thus the alignment dependence of the HHG yield again is a direct consequence of the symmetry property of their molecular orbitals.

For comparison in Fig. 2 we show the calculated alignment dependence of the ionization rates for N_2 and O_2, together with the density plots for the highest occupied molecular orbital for each of these two molecules. For O_2, clearly when the molecular axis is about 45° with respect to the laser polarization direction, its HOMO would have maximum electron density in this direction. At this angle, the tunneling ionization rate will be near the maximum and the HHG yield will also be near the maximum. For N_2, this occurs when the molecular axis is aligned with the laser polarization direction. Thus we make the general prediction that the alignment dependence of the HHG yields from molecules depends primarily on the geometry of the molecular orbitals. It should be rather insensitive to specific species, or to the laser intensity so long tunneling is the dominant ionization mechanism.

To confirm the angular dependence of the HHG predicted above, measurements have to be carried out with aligned molecules. It is best to align the molecules under the field-

free condition. This is achieved by exposing molecules to a short weak pulse to create a rotational wave packet. This wave packet rephases after the laser pulse is over and the molecules are strongly aligned periodically at intervals separated by their fundamental rotational period. In Itatani *et al.* [10], a pump pulse of intensity 4×10^{13} W/cm^2 was used to create the alignment of the N_2 molecules. At a delay time when the molecules are maximally aligned, they used a 30 fs, 3×10^{14} W/cm^2, 800 nm, horizontally polarized probe pulse to generate high-order harmonics. The angle θ between the probe and pump laser's polarizations was varied from 0 to 90°. They observed that the HHG yields decrease monotonically with increasing θ. In Fig. 3(a) we show the angular dependence of the HHG yields calculated with the present model using the laser parameters in their experiment. By assuming gas temperature of 30 K, we calculated the angular distribution $\rho(\phi, t)$ of the molecules at the time of maximal alignment when the probe laser is turned on. (Here the angle ϕ is measured from the polarization axis of the pump laser.) After convoluting with the angular distribution of the molecules, the predicted HHG yields for N_2 on the angle θ can then be compared directly with the experimental data of Itatani *et al.* Thus our results in Fig. 3(a) should be directly compared to their experimental data (their Fig. 3), both showing monotonic decrease with increasing angle θ. In their analysis of tomographic imaging of molecular orbitals of N_2, however, Itatani *et al.* assumed that all the molecules were aligned perfectly in the direction of laser polarization.

In Fig. 3(b) we show our prediction for the angular dependence for O_2 molecules if the HHG is measured in a similar pump-probe experiment. Using a 60-fs, 3×10^{13} W/cm^2, 800-nm pump laser to align O_2 molecules, the HHG yields from a 30-fs, 2×10^{14} W/cm^2 probe laser at the time of maximum alignment are shown. The predicted HHG yields increase monotonically with the angle between the two polarizations, reaching a maximum at about 45° and then decrease monotonically at larger angles. Such angular dependence in the HHG yields is expected for any molecules which have their HOMO's with π_g character. This dependence is not expected to be modified significantly by the laser parameters, nor by other finer details of the structure of the molecules.

Although the Lewenstein model has recently been used by Shan *et al.* [26] to interpret their experimental observation of the difference in the ellipticity dependence of the harmonic generation by N_2 and O_2, we note that their qualitative interpretation is incomplete. They approximated the molecular orbitals of N_2 and of O_2 as the gerade and ungerade combinations of two 1*s* atomic orbitals from the two centers, respectively, thus they would predict that in both cases the
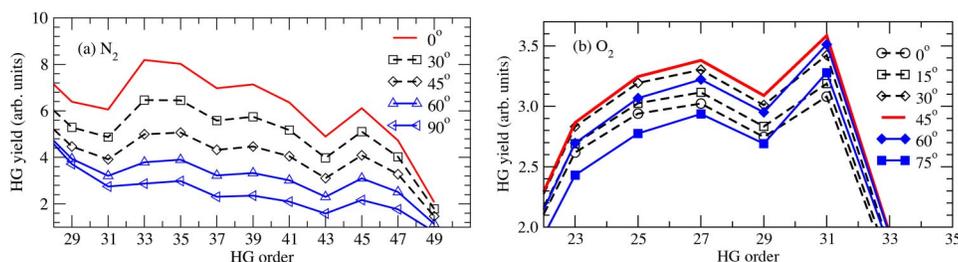
FIG. 3. (Color online) High-order harmonic yields at different angles predicted for the typical pump-probe experiments for N_2 and O_2 molecules. The angle is between the polarizations of the pump and probe lasers. The laser parameters are given in the text.

alignment dependence of the HHG peaks when the molecules are parallel to laser's polarization direction, in distinct difference from the geometric effect stressed in this paper.

Before closing we comment that the HHG yields, predicted for N_2 fixed in space, as given in Fig. 1(a), show a minimum near 60°. This minimum coincides with the zeros of the electron density plots of N_2 in Fig. 2. The position of the minimum does not change much with laser intensity. It would be interesting to see if this minimum is reproduced in future experimental HHG spectra after the effect of angular convolution is removed. If the minimum is indeed found, it would provide a firmer basis for using HHG yields for tomographic imaging of molecular orbitals, as proposed in Itatani *et al.*

In summary, we have employed accurate molecular wave functions to calculate the high-order harmonic generation in the plateau region from aligned molecules within the Lewenstein model and studied its dependence on the symmetry of the highest occupied molecular orbital. For N_2, the HHG yield is largest when the molecules are aligned in the laser polarization direction-characteristic of molecules with σ_g outermost electrons. For O_2 the HHG yield is largest when the molecular axis is about 45° with respect to the polarization axis—characteristic of molecules with π_g outermost electrons. Other recent examples showing strong orbital symmetry dependence in strong-field physics include experimental angular distributions of atomic ions after double ionization by few-cycle intense laser pulses [27,28]. From this study, we believe that continuing improvement in experimental control of the alignment and orientation of molecules [29], in combination with the measurement of harmonic yields from them, may one day prove to offer a powerful tool for imaging complex molecules.

---

[1] X. Li *et al.*, Phys. Rev. A **39**, 5751 (1989).
[2] Z. Chang *et al.*, Phys. Rev. Lett. **79**, 2967 (1997).
[3] T. Brabec and F. Krausz, Rev. Mod. Phys. **72**, 545 (2000).
[4] R. A. Bartels *et al.*, Science **297**, 376 (2002).
[5] M. Drescher *et al.*, Science **291**, 1923 (2001).
[6] M. Hentschel *et al.*, Nature (London) **414**, 509 (2001).
[7] R. Velotta *et al.*, Phys. Rev. Lett. **87**, 183901 (2001).
[8] N. Hay *et al.*, Phys. Rev. A **65**, 053805 (2002).
[9] R. de Nalda *et al.*, Phys. Rev. A **69**, 031804 (2004).
[10] J. Itatani *et al.*, Nature (London) **432**, 867 (2004).
[11] M. Lein *et al.*, Phys. Rev. Lett. **88**, 183903 (2002).
[12] M. Lein *et al.*, Phys. Rev. A **67**, 023819 (2002).
[13] J. L. Krause, K. J. Schafer, and K. C. Kulander, Phys. Rev. Lett. **68**, 3535 (1992).
[14] P. B. Corkum, Phys. Rev. Lett. **71**, 1994 (1993).
[15] M. Lewenstein *et al.*, Phys. Rev. A **49**, 2117 (1994).
[16] X. M. Tong, Z. X. Zhao, and C. D. Lin, Phys. Rev. A **66**, 033402 (2002).
[17] M. W. Schmidt *et al.*, J. Comput. Chem. **14**, 1347 (1993).
[18] X. M. Tong and S. I. Chu, Chem. Phys. **217**, 119 (1997).

[19] G. Tempea, M. Geissler, and T. Brabec, J. Opt. Soc. Am. B **16**, 669 (1999).
[20] M. Y. Ivanov, T. Brabec, and N. Bernett, Phys. Rev. A **54**, 742 (1996).
[21] C. Guo, M. Li, J. P. Nibarger, and G. N. Gibson, Phys. Rev. A **58**, R4271 (1998).
[22] M. J. DeWitt, E. Wells, and R. R. Jones, Phys. Rev. Lett. **87**, 153001 (2001).
[23] B. Shan *et al.*, Phys. Rev. A **66**, 061401 (2002).
[24] S. M. Hankin, D. M. Villeneuve, P. B. Corkum, and D. M. Rayner, Phys. Rev. Lett. **84**, 5082 (2000).
[25] J. Muth-Bohm, A. Becker, and F. H. M. Faisal, Phys. Rev. Lett. **85**, 2280 (2000).
[26] B. Shan, S. Ghimire, and Z. Chang, Phys. Rev. A **69**, 021404(R) (2004).
[27] A. S. Alnaser *et al.*, Phys. Rev. Lett. **93**, 113003 (2004).
[28] S. Voss *et al.*, J. Phys. B **37**, 4239 (2004).
[29] H. Stapelfeldt and T. Seideman, Rev. Mod. Phys. **75**, 543 (2003).